

Effect of Plasma Fluctuations on In-Flight Particle Parameters

J.F. Bisson, B. Gauthier, and C. Moreau

(Submitted 13 November 2001; in revised form 15 January 2002)

The influence of arc root fluctuations in direct current (DC) plasma spraying on the physical state of the particle jet is investigated by correlating individual in-flight particle temperature and velocity measurements with the instantaneous voltage difference between the electrodes. In-flight diagnostics with the DPV-2000 sensing device involve two-color pyrometry and time-of-flight technique for the determination of temperature and velocity. Synchronization of particle diagnostics with the torch voltage fluctuations are performed using an electronic circuit that generates a pulse when the voltage reaches some specific level; this pulse, which can be shifted by an arbitrary period of time, is used to trigger the acquisition of the pyrometric signals. Contrary to predictions obtained by numerical modeling, time-dependent variations in particle temperature and velocity due to power fluctuations induced by the arc movement can be very large. Periodic variations of the mean particle temperature and velocity, up to $\Delta T = 600$ °C and $\Delta v = 200$ m/s, are recorded in the middle of the particle jet during a voltage cycle. To our knowledge, this is the first time that large time-dependent effects of the arc root fluctuations on the particle state (temperature and velocity) are experimentally demonstrated. Moreover, large fluctuations in the number of detected particles are observed throughout a voltage cycle; very few particles are detected during parts of the cycle. The existence of quiet periods suggests that particles injected at some specific moments in the plasma are not heated sufficiently to be detected.

Keywords DPV-2000, in-flight particle diagnosis, particle temperature, particle velocity, plasma fluctuations

1. Introduction

Despite the important progress in simulation tools aimed to describe the plasma-particle interaction in the context of DC plasma spraying, experimental in-flight particle data are often not reproduced adequately. This is mainly due to the complexity of the plasma physics and also to the complex interaction between the plasma and the injected particles.^[1-5]

For example, when comparing data generated by the simulation software LAVA^[6] (Idaho National Engineering and Environmental Laboratory, Idaho Falls, ID) with experimental data obtained with NiCrAlY and zirconia used in a DC plasma spraying process, Fincke et al.^[7] obtained significant discrepancies in particle velocity and temperature, especially in the mean particle temperature ($\Delta v \approx 25$ m/s and $\Delta T \approx 1000$ °C higher than measured). No conclusive explanation was put forward, but among the possible explanations were the omission of in-flight particle evaporation, systematic error in two-color pyrometric measurement due to inaccuracy of the emissivity ratio, and lack of knowledge of the plasma physical properties that appear in the calculation. To reduce the computation time, Fincke considered the plasma steady. However, it is well known that a plasma jet issuing from a DC plasma torch displays strong fluctuations arising from the axial and rotational motion (for a swirl gas injection) of the arc root along the anode surface. This gives rise, in

the case of the restrike mode,^[8] to large (>20%) and periodic (5-20 kHz) plasma power oscillations, which might affect the in-flight particle state.

The inclusion of the arc root fluctuation phenomenon in the LAVA code was implemented soon after, and its effect on the average particle jet state was studied by Park et al.^[9] A rotationally fluctuating plasma jet was simulated by making steady-state plasma oscillate radially, while the axial component of the fluctuating plasma was simulated by applying a time-dependent input voltage to the gun. The calculation indicates that averaging over the axial fluctuations is similar to a steady plasma jet being run with the average voltage. On the other hand, the rotational fluctuations promote air-plasma mixing, which influences the plasma characteristics significantly. Still, the authors assume that the calculation can be performed adequately with equivalent steady plasma obtained by averaging the fluctuating local plasma state over the duration of a cycle. Because the time-averaged plasma conditions are fixed in time, the computation becomes easier and less time-consuming than solving for time fluctuation of electric power.

Park's simulations of a zirconia powder injected in a N₂-H₂ plasma indicate that rotational fluctuations contribute to decrease the predicted average velocity and temperature by nearly 25 m/s and 600 °C, respectively. The simulated results are in good agreement with their experimental data obtained with the DPV-2000 sensor (Tecnar Automation Ltd., St-Bruno, Quebec, Canada). This suggests that the consideration of plasma fluctuations could reconcile experimental and computed data previously generated by Fincke.

Fincke^[7] and Park^[9] assume that the moment the injection of a particle in the plasma plume takes place does not affect the resulting in-flight state of that particle. This seems reasonable, as the particle dwell time in the plasma is considered long com-

J.F. Bisson, B. Gauthier, and C. Moreau, National Research Council of Canada, Industrial Materials Institute, 75, de Mortagne Blvd, Boucherville, Quebec, Canada, J4B 6Y4. Contact e-mail: christian.moreau@cnrc-nrc.gc.ca.

pared with the fluctuation period. Nevertheless, Dussoubs et al.^[10] have shown that the spray pattern changes continuously due to arc root fluctuations, which contradicts the “large residence time” assumption. Indeed, time resolved images of the spray jet acquired with their laser strobe technique clearly showed that the spray jet trajectory varied with time delay, although no clear correlation with the power fluctuations arising from the arc root movement was demonstrated (exposure time 5 ns, separated by 30 ms, the arc root fluctuations $\approx 100 \mu\text{s}$) and no time-resolved individual in-flight particle parameter measurement was performed. Nevertheless, calculations performed with the ESTET (ensemble de simulation tridimensionnelle d'écoulements turbulents, in French)^[11] code predicted a 15% variation in the average in-flight particle velocity depending on the injection time, but nearly no change in temperature. The particle dwell time in the plasma is of the order of 1 ms, long compared with the arc root fluctuation period, which explains why small time-dependent in-flight particle velocities and temperatures were predicted.

In this article, we present (for the first time to our knowledge) time-resolved measurements of individual in-flight particle parameters. Substantial variations in particle temperature and velocity, synchronous with the voltage fluctuations, are displayed. The existence of quiet periods (around 50% of a cycle) during which very few particles are detected is also presented. This suggests that heat and kinetic energy transfers from the plasma to the particles are inefficient during some part of a cycle.

2. Experimental Set-Up

2.1 Spraying conditions

Experiments were carried out with the Sulzer-Metco F4 gun (Sulzer Metco, Westbury, NY), which uses external radial powder injection and swirl flow gas injection. Spray parameters were chosen so that the “restrike” mode is favored. This mode promotes large voltage fluctuations; it can be achieved using a low current and a high hydrogen composition in the gas mixture.^[8] Two commercial powders were used: a 7 wt.% yttria-stabilized zirconia (Amperit 825.1: +22, $-45 \mu\text{m}$, H.C. Stark, Inc., Newton, MA) and a monosized $30 \pm 5 \mu\text{m}$ alumina powder (Plasmatec PT-105C-99, Plasmatec, Inc., Montreal, Quebec, Canada). Powders having narrow particle size distributions were used to reduce size effects, which are known to enhance trajectory, temperature, and velocity variances.^[12] The powder carrier gas flow rate was chosen so as to obtain a slightly downward particle jet trajectory, which is 2 mm (4 mm) below the torch axis at a 25 mm (50 mm) stand-off distance, to obtain nearly optimal particle injection in the plasma core. 25 mm and 50 mm standoff distances were used for particle diagnostics. Constant powder feed rate (1.5 g/min) was achieved using a conventional powder feeder [Roto-feed powder hopper (Miller) model 1252, Praxair Surface Technologies, Indianapolis, IN]. Spraying conditions are summarized in Table 1.

2.2 Particle Diagnostics

In-flight particle diagnostics were carried out with the commercially available DPV-2000 sensor apparatus,^[13,14] which enables individual particle temperature (two-color pyrometry), ve-

Table 1 Experimental Spraying Conditions

Condition	Value
Powder size (μm)	Alumina: 30 ± 5 Yttria-stabilized zirconia: +22, -45
Gun	F4
Anode internal nozzle diameter (mm)	7
Current (A)	550
Powder (kW)	37
Primary gas flow rate (Ar) (l/min)	35 (swirl flow injection)
Secondary flow rate (H ₂) (l/min)	10
Carrier gas flow rate (Ar) (l/min)	1.7 (ZrO ₂) 3.0 (Al ₂ O ₃)
Powder feeder	Roto-feed powder hopper (Miller) model 1252
Powder feed-rate (g/min)	1.5
Injection type	External
Stand off distance (mm)	ZrO ₂ : 25-50 Al ₂ O ₃ : 50

locity (time of flight method), and diameter (absolute intensity corrected for velocity and temperature) measurements. Unless mentioned otherwise, diagnosis was performed in the middle of the jet (transverse field of view: $110 \mu\text{m} \times 300 \mu\text{m}$, depth of field: 2 mm), where particle flow rate is at a maximum.

To reduce the effect of velocity dispersion on the effective time-resolution (see Section 4), particle sensing was performed as close to the nozzle exit as possible without overly degrading the quality of the measurements due to plasma radiation. In effect, at a short distance from the torch exit, the visibility of the particle radiative signal is reduced due to fluctuations of the plasma background.^[15] Thus, diagnostics were performed just far enough from the nozzle exit to avoid direct collection of the plasma light. Also, particles were hot enough for the plasma light scattered by the particles to be of negligible influence on the temperature estimate.^[16]

2.3 Time-Resolved Diagnostics With the DPV-2000

When the DPV-2000 is used in normal conditions, the acquisition of the pyrometric signals is triggered when the pyrometric signal in one channel exceeds a predefined threshold. In this work, the signal used to trigger the acquisition of the in-flight particle signal was no longer a particle radiation signal, but the torch voltage. The principle of operation of the synchronization system is sketched in Fig. 1 and can be summarized as follows.

The time-dependent voltage signal was measured by electrical contacts on the cathode and the anode of the plasma torch. The voltage was then sent to an analog comparator circuit; the circuit output being a positive pulse when the torch voltage signal exceeds a predefined value. Using a time delay generator, the resulting pulse could be digitally shifted by an adjustable delay before sending it to the trigger input of the acquisition card. Each acquisition lasted 20 μs . When a particle passed into the sensor's field of view during that period, it could be analyzed and its temperature, velocity, and diameter extracted. For each time delay, measurements were repeated until a statistically significant number of particles was analyzed; that is, at each time step a sample size larger than 300 is grabbed, except when the count rate is too small to enable a valid measurement within a reason-

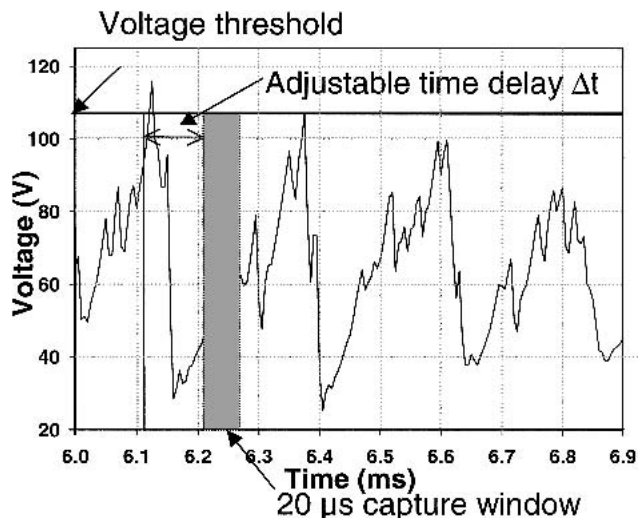


Fig. 1 Principle of operation of the synchronization of the diagnostics with the torch voltage

able delay. The time delay was varied to probe the entire period of the torch voltage fluctuations.

As shown in Fig. 1, the voltage behavior was *nearly periodic* with a fundamental period of around $225 \mu\text{s}$. It also displayed an irregular “saw-tooth” behavior inside each $225 \mu\text{s}$ cycle. Due to the irregular behavior of the torch voltage inside each cycle (Fig. 1), an arbitrary threshold for the comparator would have led to significant voltage phase uncertainty. To get around that problem, the threshold was selected to be as high as possible (around 110 V), so only when the voltage exceeded that value did the comparator circuit generate a pulse that triggered the signal acquisition. This not only enabled suitable phase resolution¹ from particle to particle, but as will be seen, also allowed us to detect in-flight particle modulation due to the 360 Hz ripple. The latter generally arises from the rectification of the three phases of the AC 60 Hz voltage, which are out of phase by 120° .

3. Results

Mean particle temperatures and velocities obtained in the center of the jet at 50 mm from the torch exit are shown for the alumina case in Fig. 2(a) and (b) as a function of time delay. Error bars are the 1σ confidence interval on the mean value. Numerical values on the graph are the sample standard deviation. Periodic variations of the average particle temperature and velocity, reaching nearly 500°C and 200 m/s , were obtained for alumina. The period of the cycles coincides with that of the voltage fluctuations (period $\approx 220 \mu\text{s}$, or $f \approx 4500 \text{ Hz}$).

A summary of particle temperature and velocity data obtained with alumina and zirconia is shown in Table 2. It should be noted that the observed amplitude of variations decreases with stand-off distance, as can be seen by comparing results obtained at 25 mm and 50 mm for zirconia. This is due to velocity

¹The phase resolution needs not be significantly better than the phase uncertainty arising from the capture depth of the sensor ($20 \mu\text{s}$, i.e., 30° uncertainty).

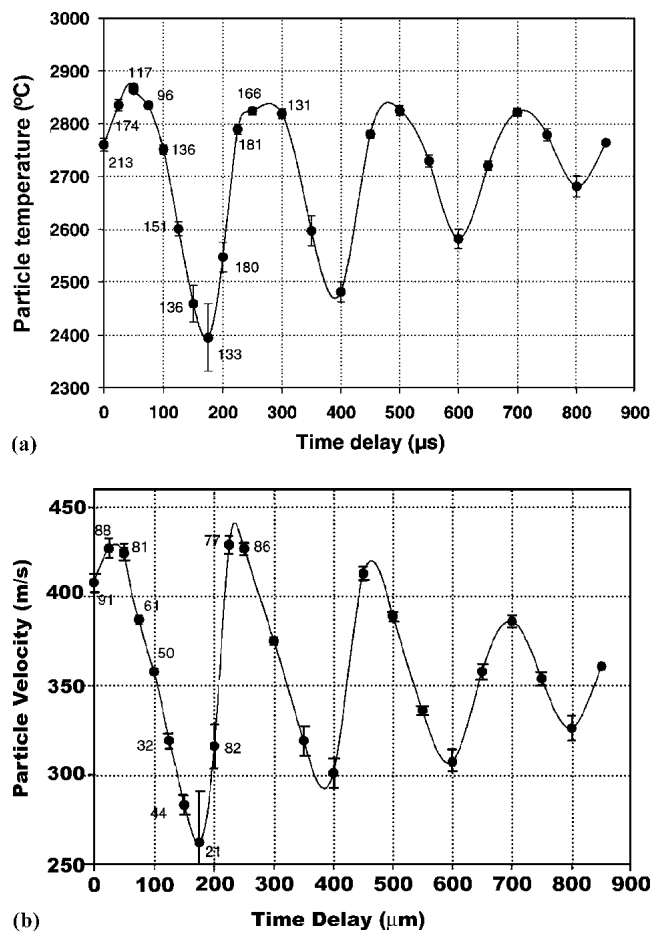


Fig. 2 (a) Fluctuation of the temperature of alumina particles as a function of time delay. Error bars are the 1σ confidence interval on the mean value. Numerical data are the sample standard deviations. (b) Fluctuation of the average velocity of alumina particles as a function of time delay. Error bars are the 1σ confidence interval on the mean value. Numerical data are the sample standard deviations.

dispersion, which produces a time-of-flight broadening from the injection to the sensing location proportional to the traveled distance. This causes a reduction in the effective time-resolution of the diagnostics when extrapolated at the injection point (see Section 4). Hence, diagnostics were performed as close to the injection point as possible.

The number of detected particles per unit time is shown as a function of time delay in Fig. 3. The maximum particle flow rate, observed at $\Delta t = 100 \mu\text{s}$, is shifted with respect to the maxima in velocity and temperature values (observed at $\Delta t = 50 \mu\text{s}$, Fig. 2a,b). Note that almost no particle is detected during some parts of each cycle. The existence of quiet periods suggests that particles that are injected at some specific moments in the plasma are either not heated or propelled efficiently by the plasma jet.

To evaluate the extent of particle jet trajectory fluctuations due to plasma fluctuations, the jet was scanned vertically by the DPV-2000 sensor at two specific time delays ($100 \mu\text{s}$ and $200 \mu\text{s}$) corresponding to maximum and minimum detection rate. The particle detection rate values as a function of vertical position of the sensor are shown in Fig. 4 for these time delays. The ampli-

tude of variation of the jet orientation during a cycle, as evaluated from the position where the maximum detection rate is obtained, is only about 2 mm. Hence, it seems that the particles injected “at the wrong time” do not simply change their trajectory, as suggested in previous work,^[10] but are too cold to be detected pyrometrically.

Finally, the 360 Hz component arising from the ripple due to the rectification of the three 60-Hz phases also induces a modulation of the average temperature on the millisecond (ms) time scale, i.e., period $T = 2.78$ ms, as can be seen in Fig. 5 where a variation corresponding to a period of the order of a few ms appears to emerge.

Table 2 A Summary of the Results of the Diagnostics for Alumina and Zirconia and Two Stand-off Distances for the Litter

Particle Type and Distance	Amplitude of Temperature Variations, °C	Amplitude of Velocity Variations, m/s	Mean Temperature and Sample SD, °C, Averaged Over One Cycle	Mean Velocity and Sample SD, °C, Averaged Over One Cycle
Alumina, 50 mm	500	200	2761 ± 184	380 ± 80
Zirconia, 25 mm	383	60	2840 ± 266	192 ± 41
Zirconia, 50 mm	160	27	2861 ± 216	206 ± 39

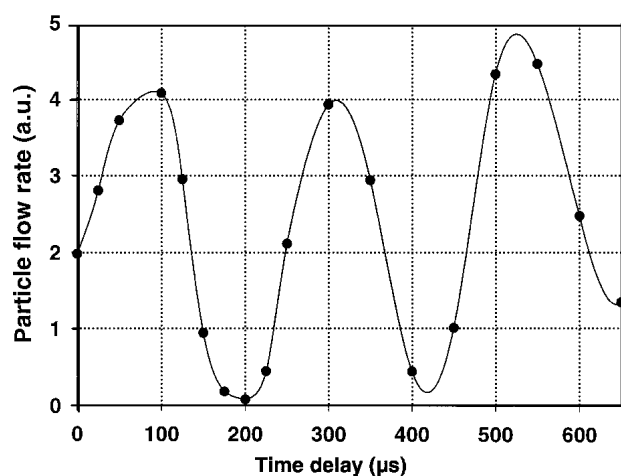


Fig. 3 Fluctuation of the alumina particle flow rate as a function of time delay. Periods during which almost no particle are detected are noticeable around $t = 200 \mu\text{s}$ and $t = 400 \mu\text{s}$.

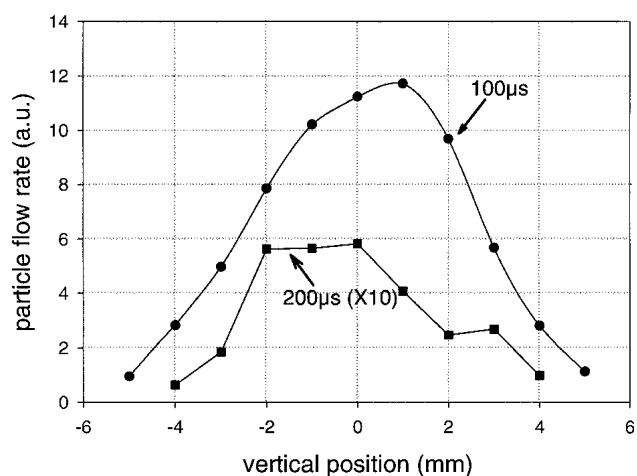


Fig. 4 Vertical flow rate profile (alumina) at $t = 100 \mu\text{s}$ and $t = 200 \mu\text{s}$. The latter curve is magnified by a factor 10 for better visibility.

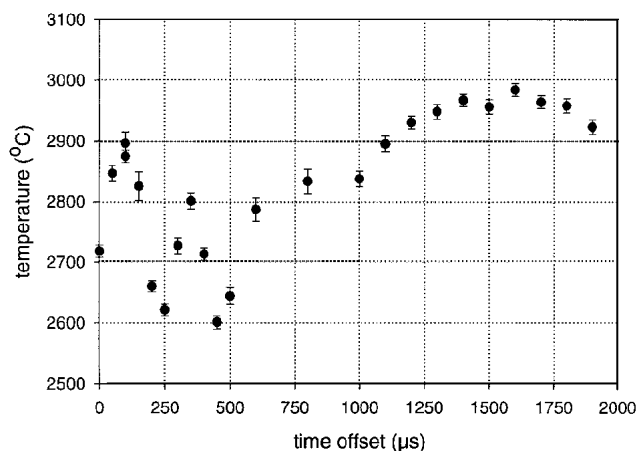


Fig. 5 Time evolution of the average temperature. A periodic evolution of the average temperature on the ms range probably corresponds to a 360 Hz ripple arising from the rectifying of the three “60 Hz” phases. The error bars indicate the 1σ confidence interval on the mean value.

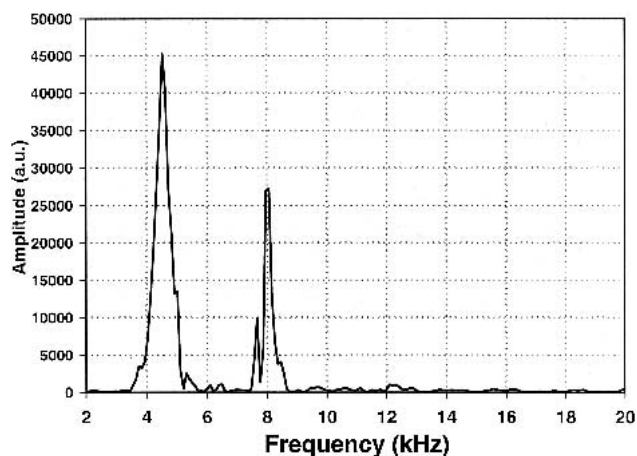


Fig. 6 Amplitude spectrum of the voltage signal. Two peaks around 4.5 and 8 kHz are clearly visible. The peak finesse, defined as the ratio of the peaks position over peak width, is about 10. It indicates that the phase reference is conserved for a few cycles.

4. Discussion

4.1 Influence of the Finite Coherence of the Voltage Fluctuations on the Time-Resolved Diagnostics

A gradual decrease in the amplitude of the cycles as a function of time delay is noticeable in Fig. 2(a) and (b). This can be understood by considering the Fourier amplitude spectrum of the voltage fluctuations, of which a portion is shown in Fig. 6. The nonzero width (around 500 Hz) of the 4.5 kHz peak indicates the nonperfect periodicity of the voltage evolution, resulting in a gradual loss of coherence after a few cycles. In other words, knowing the voltage at some time $V(t=0)$, the future state of the voltage $V(t)$ can only be predicted to some extent within a few cycles away from the origin; beyond a certain period t , $V(t)$ becomes uncorrelated with $V(t=0)$. Therefore, if n particles, each corresponding to different realizations of $V(t)$, are analyzed at a large time delay, we expect the resulting values to be time-averaged values because the synchronization is lost.

Note that the energy transfer to a particle depends on the input power (or voltage) in the plasma jet *during its dwell time* in the plasma. A particle analyzed at time delay Δt_0 after the peak voltage (Fig. 1) will have a temperature and velocity determined by the voltage behavior prior to the measurement, due to the time of flight of the analyzed particle from its injection into the plasma to the sensor location. Hence, particles that are detected at zero time delay do not necessarily correspond to those being injected when the plasma is in the highest energy. In the case of alumina, the measured particle in-flight velocity is nearly 400 m/s, the stand-off distance is 50 mm, and assuming a uniform acceleration from the injector to the sensor field of view, the total time of flight is about: $50 \cdot 10^{-3} \text{ m} / 200 \text{ m/s} \approx 250 \mu\text{s}$, which is comparable to the period of a cycle. A more accurate estimate of the time of flight would require careful modeling of the complex interaction between the plasma and the injected particles. Therefore, the time delays in Fig. 2 and 3 should be viewed in a relative sense.

It is noteworthy that the velocity dispersion has nothing to do with the gradual decrease in the amplitude of the oscillations with Δt . However, velocity dispersion does contribute to reduce the amplitude of the oscillations as the distance between the sensor and the injector increases as shown in Table 2 for zirconia.

4.2 Influence of Plasma Fluctuations on the Statistical Variance of the In-Flight Particle Characteristics

The large fluctuations in temperature and velocity displayed in Fig. 2(a) and (b) suggest that the plasma fluctuations contribute to significantly increase the statistical variance of in-flight particle temperature and velocity (see Table 2). However, this assertion is mitigated by the number of detected particles (Fig. 3), which is significant only during a fraction of the cycle. Nevertheless, particle temperature and velocity vary over 250 °C and 100 m/s (for alumina) during that part of the cycle, that is, between $\Delta t = 50 \mu\text{s}$ and $\Delta t = 125 \mu\text{s}$. Considering the time-averaged dispersion in velocity and temperature, it appears that plasma fluctuations are a prime source of broadening of the in-flight particle velocity and temperature distributions. Other phenomena, such as aerodynamic size effect, dispersion in injection ve-

locity, and injection direction and turbulence also play an important role in the statistical broadening of the in-flight particle state^[12] and explain some of the dispersion measured at a specific time delay.

The fact that a small number of particles is detected during some portion of a cycle suggests that some particles are not heated enough to be detected in the sensor area during that portion of the cycle. If this were indeed the case, then the actual dispersion of temperature and velocity would be larger than it appeared because the cold particles, which were not accounted for, would contribute to broaden the temperature distribution. Another scenario is that particles that are injected when the plasma is less energetic do not have time to bypass the nozzle and are caught up when the next hot puff of plasma comes out, giving rise to puffs of hot particles. A combination of these two scenarios is also possible. Laser illumination of the particles would make it possible to count the cold particles and will be a useful tool to get a better picture of physical mechanisms underlying the particle-plasma jet interaction.

Note that the amplitude of the variation in the in-flight particle state depends on the amplitude of the fluctuation $V(t)$ as well as on how the particle dwell time in the plasma compares with the duration of a cycle. The experimental conditions chosen in this work were such that these two conditions are favored. The spray gun conditions were chosen to favor the restrike mode, and the powders that were used both displayed small particles, thus favoring a shorter residence time in the plasma. Alumina particles displayed larger time-dependent variations than zirconia because they are lighter, and therefore, spend less time in the plasma.

5. Conclusion

The influence of the plasma fluctuations on the in-flight particle state was evaluated by synchronizing the particle diagnostics with the torch voltage. Time-dependent particle temperature and velocity variations due to arc fluctuations, as large as $\Delta T = 600 \text{ }^\circ\text{C}$ and $\Delta v = 200 \text{ m/s}$, were observed. Plasma fluctuations were found to be a prime source of statistical variance in the in-flight particle velocity and temperature. Moreover, very few particles were detected in a portion of a cycle. To our knowledge, this is the first time large effects of arc root fluctuations on particle state (temperature, velocity, and number of particles) are established. Note, however, that spraying conditions used in production might be far less favorable to the presence of large fluctuations, so the extent to which plasma fluctuations affect the particle behavior is strongly process dependent.

How the particles interact with a fluctuating plasma jet needs to be better understood. Work is under way to gain some understanding of the particle jet behavior in a plasma jet. Particle illumination with lasers is a tool that will allow us to see some cold particles that go undetected by pyrometric means. Using simulation tools that model the interaction of the particles with the plasma jet will also help to get a better picture of behavior of the particle jet.

Acknowledgment

Useful discussions with S. Goergaris, L. Pouliot, J. Blain, and F. Nadeau from Tecnar Automation are deeply acknowledged. Proofreading by Rogerio Lima is also much appreciated.



References

1. M. Vardelle, A. Vardelle, P. Fauchais, and M.I. Boulos: "Plasma-Particle Momentum and Heat Transfer: Modeling and Measurements," *AIChE J.*, 1983, 29(2), pp. 236-43.
2. R. Ye, P. Proulx, and M. Boulos: "Turbulence Phenomena in the Radio Frequency Induction Plasma Torch," *Int. J. Heat Mass Transfer*, 1999, 42, pp. 1585-95.
3. P. Fauchais, J.F. Coudert, and M. Vardelle: "Transient Phenomena in Plasma Torches and in Plasma Sprayed Coating Generation," *J. Phys. IV France*, 1997, 7, pp. C4-187 to C4-198.
4. J.F. Coudert, M.P. Planche, and P. Fauchais: "Anode-Arc Attachment Instabilities in Spray Plasma Torch," *High Temp. Chem. Process.*, 1994, 3, pp. 639-51.
5. J.F. Coudert, M.P. Planche, and P. Fauchais: "Characterization of D.C. Plasma Torch Voltage Fluctuations," *Plasma Chem. Plasma Process.*, 1996, 16(1), pp. 211S-27S.
6. C.H. Chang and J.D. Ramshaw: "Computational Fluid Dynamics Modeling of Multicomponent Thermal Plasmas," *Plasma Chem. Plasma Process.*, 1992, 12, pp. 299-325.
7. J.R. Fincke, R.L. Williamson, and C.H. Chang: "Plasma Spraying of Functionally Grade Materials, Measured and Simulated Results" in *Thermal Spray: Surface Engineering Via Applied Research*, ASM International, Materials Park, OH, 2000, pp. 141-148.
8. Z. Duan and J. Heberlein: "Anode Boundary Layer Effects in Plasma Spray Torches" in *Thermal Spray: Surface Engineering Via Applied Research*, ASM International, Materials Park, OH, 2000, pp.1-7.
9. J.H. Park, J. Heberlein, E. Pfender, Y.C. Lau, J. Ruud, and H.P. Wang: "Particle Behavior in Fluctuating Plasma Jet," *Ann. N.Y. Acad. Sci.*, 1999, 891, pp. 417-24.
10. B. Dussoubs, G. Mariaux, A. Vardelle, M. Vardelle, and P. Fauchais: "D.C. Plasma Spraying, Effect of Arc Root Fluctuations on Particle Behavior in the Plasma Jet," *High Temp. Material Process.*, 1999, 3, pp. 235-50.
11. J.D. Mattei and O. Simonin: *Logiciel ESTET. Manuel Theorique de la Version 3.1.*, EDF Report HE 44/92.38b, 1992 (in French).
12. R.L. Williamson, J.R. Fincke, and C.H. Chang: "A Computational Examination of the Sources of Statistical Variance in Particle Parameters During Thermal Plasma Spraying" in *Surface Engineering Via Applied Research*, C.C. Berndt, ed., ASM International, Materials Park, OH, 2000, pp. 115-24.
13. P. Gougeon, C. Moreau, V. Lacasse, M. Lamontagne, I. Powell, and A. Bewsher: "A New Sensor for On-Line Diagnostics of Particles Under Thermal Spraying Conditions" in *Adv. Process. Tech., Particulate Materials*, 6, Metal Powder Industries Federation, Princeton, NJ, 1994, pp. 199-210.
14. J. Blain, F. Nadeau, L. Pouliot, C. Moreau, P. Gougeon, and L. Leblanc: "Integrated Infrared Sensor System for On-Line Monitoring of Thermally Sprayed Particles," *Surf. Eng.*, 13, 1997, pp. 420-24.
15. T. Sakuta and M.I. Boulos: "Novel Approach for Particle Velocity and Size Measurement Under Plasma Conditions," *Rev. Sci. Instrum.*, 1988, 59(2), pp. 285-91.
16. P. Gougeon and C. Moreau: "In-Flight Particle Surface Temperature Measurement: Influence of the Plasma Light Scattered by the Particles," *J. Therm. Spray Technol.*, 1993, 2(3), pp. 229-33.